2-Acetylthiamin Pyrophosphate (Acetyl-TPP) pH–Rate Profile for Hydrolysis of Acetyl-TPP and Isolation of Acetyl-TPP as a Transient Species in Pyruvate Dehydrogenase Catalyzed Reactions†

Kenneth J. Gruys, Asit Datta, and Perry A. Frey*

Institute for Enzyme Research, The Graduate School, and Department of Biochemistry, College of Agricultural and Life Sciences, University of Wisconsin—Madison, Madison, Wisconsin 53705

Received April 25, 1989; Revised Manuscript Received July 6, 1989

ABSTRACT: Rate constants for the hydrolysis of acetyl-TPP were measured between pH values of 2.5 and 7.5 and plotted as log k_{obs} versus pH. The pH–rate profile defined two legs, each with a slope of +1 but separated by a region of decreased slope between pH 4 and pH 6. The rates were insensitive to buffer concentrations. Each leg of the profile reflected specific-base-catalyzed hydrolysis of acetyl-TPP, analogous to the hydrolysis of 2-acetyl-3,4-dimethylthiazolium ion [Lienhard, G. E. (1966) *J. Am. Chem. Soc. 88*, 5642–5649]. The separation of the two legs of this profile has been shown to be caused by the ionization of a group exhibiting a pK_a of 4.73 within acetyl-TPP that is remote from the acetyl group, the aminopyrimidine ring, which is protonated below pH 4.73. The protonation level of this ring has been shown to control the equilibrium partitioning of acetyl-TPP among its carbinolamine, keto, and hydrate forms. The differential partitioning of these species is a major factor causing the separation between the two legs of the pH–rate profile. The characteristic pH–rate profile and the availability of synthetic acetyl-TPP [Gruys, K. J., Halkides, C. J., & Frey, P. A. (1987) *Biochemistry 26*, 7575–7585] have facilitated the isolation and identification of [1-^{14}C]acetyl-TPP from acid-quenched enymatic reaction mixtures at steady states. [1-^{14}C]Acetyl-TPP was identified as a transient species in reactions catalyzed by the PDH complex or the pyruvate dehydrogenase component of the complex (E_1). The pH–rate profile for hydrolysis of [1-^{14}C]-acetyl-TPP isolated from enzymatic reactions was found to be indistinguishable from that for authentic acetyl-TPP, which constituted positive identification of the ^{14}C-labeled enzymic species.

2-Acylthiazolium salts are known to undergo acyl group transfer reactions with nucleophiles (Breslow, 1958; White & Ingraham, 1960, 1962; Breslow & McNelis, 1960; Daigo & Reed, 1962; Lienhard, 1966). Several reactions catalyzed by TPP[1]-dependent enzymes catalyze acyl group transfers that may involve species of acyl-TPP as intermediates. Acetyl-TPP, for example, is regarded as very likely to be an intermediate in the phosphoketolase reaction. This possibility is supported but not proven by studies of phosphoketolase (Schroter & Holzer, 1963; Goldberg & Racker, 1962). Early studies of α-keto acid dehydrogenase complexes gave results that could be interpreted in terms of the involvement of intermediates such as acetyl-TPP (Das et al., 1961; da Fonseca-Wollheim et al., 1962). And recent findings in this laboratory indirectly implicate acetyl-TPP and succinyl-TPP as intermediates in certain reactions catalyzed by α-keto acid dehydrogenase complexes, which are related to but not identical with the overall α-keto acid dehydrogenation reactions (Steginsky & Frey, 1984; CaJacob et al., 1985; Flournoy & Frey, 1986).

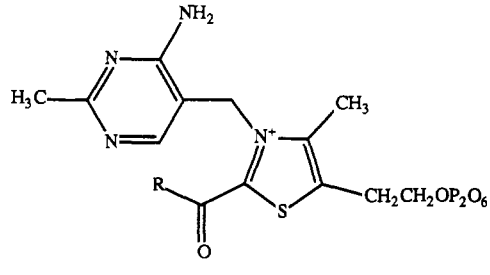

acyl-TPP

The overall reaction catalyzed by the pyruvate dehydrogenase complex (PDH complex) is equation 6, and it proceeds by the reaction sequence shown in eq 1–5. The many

$$CH_3COCO_2^- + E_1\cdot TPP + H^+ \rightarrow E_1\cdot CH_3C(OH){=}TPP + CO_2 \quad (1)$$

$$E_1\cdot CH_3C(OH){=}TPP + E_2\text{–}lipS_2 \rightleftharpoons E_1\cdot TPP + E_2\text{–}lip(SH)SCOCH_3 \quad (2)$$

$$E_2\text{–}lip(SH)SCOCH_3 + CoASH \rightleftharpoons E_2\text{–}lipoyl(SH)_2 + CH_3COSCoA \quad (3)$$

$$E_2\text{–}lip(SH)_2 + E_3\cdot FAD \rightleftharpoons E_2\text{–}lip(S)_2 + E_3\cdot FADH_2 \quad (4)$$

$$E_3\cdot FADH_2 + NAD^+ \rightleftharpoons E_3\cdot FAD + NADH + H^+ \quad (5)$$

$$\text{sum: } CH_3COCO_2^- + CoASH + NAD^+ \rightarrow CO_2 + CH_3COSCoA + NADH \quad (6)$$

mechanisms that may be considered for the TPP-mediated reductive acetylation of E_2–$lipS_2$ in eq 2 can be grouped into those that follow pathways A and B in Scheme I. Pathway

† This research was supported by Grant AM 28607 from the National Institute of Diabetes and Digestive and Kidney Diseases. K.J.G. was supported by a postdoctoral fellowship awarded by the National Institute of General Medical Sciences, Grant GM 10816.

[1] Abbreviations: E_1, pyruvate dehydrogenase; E_2, dihydrolipoyl transacetylase; E_3, dihydrolipoyl dehydrogenase; TPP, thiamin pyrophosphate; hydroxyethyl-TPP, 2-(1-hydroxyethyl)thiamin pyrophosphate; lactyl-TPP, 2-(1-carboxy-1-hydroxyethyl)thiamin pyrophosphate; hydroxyethylidene-TPP, 2-(1-hydroxyethylidene)thiamin pyrophosphate; acyl-TPP, 2-acylthiamin pyrophosphate; acetyl-TPP, 2-acetylthiamin pyrophosphate; succinyl-TPP, 2-succinylthiamin pyrophosphate; FAD, flavin adenine dinucleotide; CoA, coenzyme A; NAD^+ and NADH, nicotinamide adenine dinucleotide, oxidized and reduced forms, respectively; TCA, trichloroacetic acid; NMR, nuclear magnetic resonance; EDTA, ethylenediaminetetraacetic acid; GTP, guanosine 5′-triphosphate; MES, 2-(*N*-morpholino)ethanesulfonic acid; MOPS, 3-(*N*-morpholino)-propanesulfonic acid; PMSF, phenylmethanesulfonyl fluoride.

0006-2960/89/0428-9071$01.50/0

Scheme I

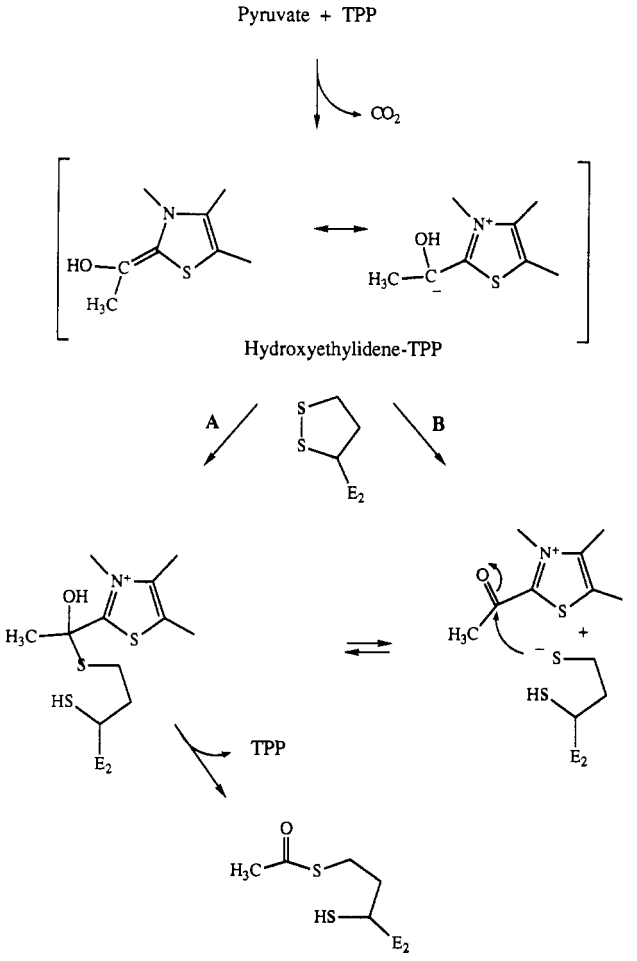

A refers to mechanisms in which oxidation–reduction and group transfer are tightly coupled and occur simultaneously as different manifestations of the same chemical steps. Pathway B refers to mechanisms in which the oxidation–reduction and group transfer proceed in distinctly different steps. Pathway B is initiated by the oxidation of hydroxyethylidene-TPP to acetyl-TPP and the reduction of lipoamide to dihydrolipoamide, followed by acetyl group transfer to form TPP and S^8-acetyldihydrolipoamide. Both pathways are assumed to involve the intermediate tetrahedral adduct formed between acetyl-TPP and dihydrolipoamide.

Pathways A and B in Scheme I differ by the *compulsory* involvement of acetyl-TPP in pathway B and not in pathway A. If acetyl-TPP can be shown not to be present during the overall reaction, all mechanisms that follow pathway B can be excluded. Currently available evidence implicating acetyl-TPP as an enzymic intermediate is indirect and inconclusive. We are, therefore, investigating the properties of acetyl-TPP and its possible involvement in reactions catalyzed by the PDH complex.

We recently described the synthesis, characterization, and some of the properties of acetyl-TPP (Gruys et al., 1987). As expected, based on the properties of 2-acetyl-3,4-dimethylthiazolium ion (Lienhard, 1966), ketonic and hydrated forms of acetyl-TPP were identified in acidic aqueous solutions. However, we also observed a third species formed by the intramolecular addition of the pyrimidinyl amino group to the carbonyl group of the 2-acetylthiazolium moiety (Gruys et al., 1987). This carbinolamine form, shown in Scheme II, was found to be in equilibrium with the keto and hydrate forms of the molecule.

Scheme II

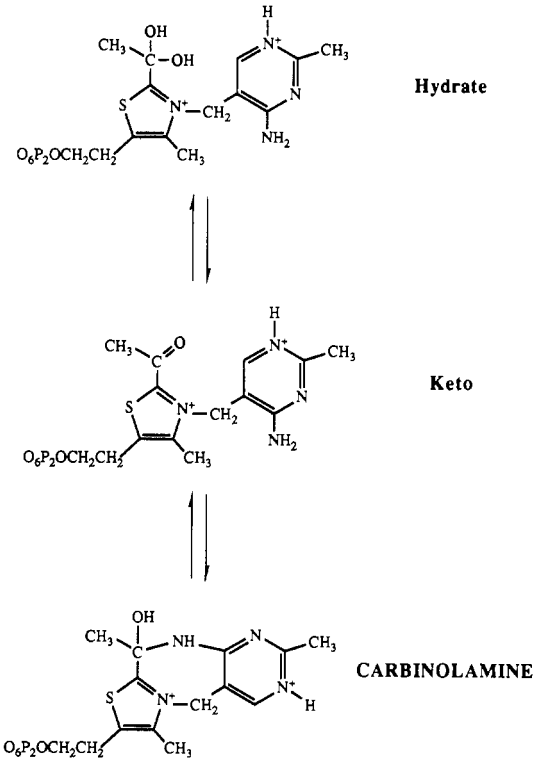

In this paper we present the results of the further chemical characterization of acetyl-TPP, with particular reference to the pH–rate profile for its hydrolysis. The presence of the pyrimidine ring and the carbinolamine form of the molecule profoundly affects the pH dependence for hydrolysis as compared with the model compound 2-acetyl-3,4-dimethylthiazolium ion studied by Lienhard (1966). We also describe the isolation and characterization of [1-^{14}C]acetyl-TPP from quenched enzymic reaction mixtures containing the substrates [2-^{14}C]pyruvate or [1-^{14}C]acetyl-CoA.

Experimental Procedures

Materials. Chemicals, coenzymes, enzymes, and chromatographic materials were purchased from the following commericial sources: TPP, GTP, CoA, NAD^+, and Sephadex SP-C25 from Sigma; P6DG desalting gel and the anion-exchange resin AG1-X4 from Bio-Rad; potassium ferricyanide, trichloroacetic acid, sodium formate, sodium acetate, monobasic sodium phosphate, MOPS, MES, sodium 3-(trimethylsilyl)-1-propanesulfonate, D_2O, and DCl from Aldrich; [2-^{14}C]pyruvate from New England Nuclear; [1-^{14}C]acetyl-CoA from Amersham. Scintillation cocktail was Bio-Safe II (Research Products International). All other chemicals were of highest available purity from readily available sources and were used as supplied by the vendors.

The PDH complex and the pyruvate dehydrogenase component (E_1) were purified by published procedures (Reed & Willms, 1966; Speckhard & Frey, 1975). Likewise, the α-ketoglutarate dehydrogenase complex and the E_2E_3 subcomplex of the α-ketoglutarate dehydrogenase complex were isolated as described elsewhere (Reed & Mukherjee, 1969; Pettit et al., 1973). Minor modifications included the addition of 1 mM EDTA and 1 mM PMSF in all purification steps to minimize proteolysis, the addition of 1% RNA at pH 6.2 to the buffer used to redissolve the protamine sulfate pellet (0.007 times the volume of crude extract), and beginning the isoelectric fractionation to separate α-ketoglutarate and PDH complexes at pH 5.9 instead of 5.7, with the pH being reduced

in 0.2 pH increments. Pyruvate dehydrogenase (E_1) and the E_2E_3 subcomplex of the α-ketoglutarate dehydrogenase complex were combined to form a hybrid complex as described by Steginsky et al. (1985). Synthetic acetyl-TPP was prepared and stored as previously described (Gruys et al., 1987). [1-^{14}C]Acetyl-CoA was purified as outlined by Flournoy and Frey (1986) and CaJacob et al. (1985) and diluted with carrier to the desired specific radioactivity (between 15 and 20 μCi/μmol). [2-^{14}C]Pyruvate was first diluted with carrier to a specific activity of 5–10 μCi/μmol and then purified prior to use by anion-exchange chromatography using the resin Bio-Rad AG1-X4 (Cl^-). Five milliliters of sample was loaded onto the column (1.0 × 17 cm, washed and equilibrated with H_2O) at neutral pH and then eluted in steps with HCl as follows: H_2O, 25 mL; 6 mM HCl, 35 mL; 30 mM HCl, 75 mL; and 100 mM HCl, 35 mL. Acetic acid emerged in the 6 mM wash, pyruvic acid in the 30 mM wash, and parapyruvate and other aldol addition products in the 100 mM wash. Pooled fractions of pure [2-^{14}C]pyruvate were adjusted to pH 4.0, concentrated by flash evaporation, and stored at −70 °C.

Instrumentation. The rates of hydrolysis of synthetic acetyl-TPP and spectral measurements in general were performed by using a Cary 118 UV–vis spectrophotometer equipped with a temperature-controlled circulating water bath. Radioactivity (^{14}C) was measured by using a Packard Tri-Carb Model 4640 scintillation spectrometer set to the ^{14}C window (93% efficiency). Proton NMR spectra were obtained by using a Bruker WH-270 spectrometer field frequency locked on the deuterium resonance of 99.8 atom % D_2O. Chemical shifts are reported downfield from sodium 3-(trimethylsilyl)-1-propanesulfonate (internal).

Volatile Transfer. Volatile transfer of [1-^{14}C]acetic acid produced in the hydrolysis of [1-^{14}C]acetyl-TPP was accomplished by using a V-shaped glass vessel (approximately 1 cm i.d. × 10 cm in length per arm) with a single outlet on top for connection to a vacuum pump. The outlet was regulated by a well-greased stopcock. Complete transfer of known amounts of acetic acid in analytical test reactions was confirmed by assaying the components collected by volatile transfer using acetate kinase and hydroxylamine as described by Rose et al. (1954) and modified by CaJacob et al. (1984). The acetohydroxamate produced was detected by measurement of A_{540} after reaction with acidic $FeCl_3$ (Lipmann & Tuttle, 1945). Additional confirmation of complete acetic acid transfer was obtained by monitoring the rate of acetate production from the hydrolysis of synthetic acetyl-TPP. The hydrolysis rate at pH 6.2 measured by this procedure gave the same rate constant as that found by following the decrease in A_{310} (see below).

Trapping of Enzymatic Reaction Intermediates. The trapping of [1-^{14}C]acetyl-TPP and other ^{14}C-labeled TPP reaction intermediates was accomplished by quenching enzymatic reactions of ^{14}C-labeled substrates with acid during the steady state. Each reaction was carried out in the presence of 50 mM bicine at pH 8.1 and was quenched by the addition of 100 μL of 20% TCA followed by 100 μL of 15 mM synthetic acetyl-TPP. Acetyl-TPP was added as carrier to aid in the identification of acetyl-TPP-containing fractions after chromatography of the reaction mixture. The exact reaction conditions and the time of the quench varied with the system under examination and is described below for each system.

The conversion of [2-^{14}C]pyruvate to [1-^{14}C]acetyl-CoA by the action of the PDH complex was quenched in the steady state. The PDH complex (6 mg) was incubated with 0.4 μmol of TPP, 2 μmol of CoA, 2 μmol of NAD^+, and 1 μmol of $MgSO_4$ for 15 min at 4 °C in a volume of 837 μL. To initiate the reaction, 2 μmol of [2-^{14}C]pyruvate in 163 μL of water at 4 °C was added. The reaction was quenched after approximately 2 s. A second experiment was performed as above in the additional presence of 0.5 mM GTP, a noncompetitive inhibitor against the substrate pyruvate. The GTP was added in the preliminary incubation step. Two control experiments with PDH complex were carried out as above except that TPP was omitted in one case and CoA in the other.

The same reaction as above catalyzed by the PDH complex (minus GTP) was carried out under anaerobic conditions. Distilled water was boiled for 10 min, cooled by purging with argon, and sealed under vacuum. Concentrated (1.6 M) sodium bicinate buffer at pH 8.6 was diluted with the oxygen-free water to give 150 mM buffer at pH 8.1. Cofactors, in amounts equivalent to those used under aerobic conditions, were dissolved in the O_2-free buffer and kept sealed in a 1-mL glass vial covered with a rubber septum. The vessel was flushed with argon for 15 min. Enzyme was then added, and the vial was immersed in an ice–water bath at 4 °C while argon was passed gently through the reaction vessel. Into an identical vial [2-^{14}C]pyruvate was added at the same level of radioactivity and concentration as in the aerobic reaction. The [2-^{14}C]pyruvate solution was purged with argon for 15 min, and the reaction was started by anaerobically transferring the [2-^{14}C]pyruvate via a syringe while argon was passed continuously through the reaction vessel. The reaction was quenched after 2 s of reaction time.

In a reaction catalyzed by the E_1 component of the PDH complex, the presence of acetyl-TPP was tested with O_2 as the only electron acceptor. Six milligrams of the PDH complex, 0.4 μmol of TPP, and 1.0 μmol of $MgCl_2$ in a volume of 837 μL were gently oxygenated with bubbling O_2 for 5 min at room temperature. To this was added 2 μmol of [2-^{14}C]pyruvate in 163 μL of water to initiate the reaction. After 30 s, the reaction was quenched.

Pyruvate dehydrogenase (E_1) catalyzed oxidative decarboxylation of pyruvate with ferricyanide as the redox reagent was examined for steady state levels of acetyl-TPP. Purified E_1 was concentrated by ammonium sulfate precipitation prior to carrying out the reaction. The concentrated E_1 (5.4 mg) was incubated for 5 min at room temperature with 0.4 μmol of TPP and 1.0 μmol of $MgCl_2$ in a volume of 804 μL. To this was added 4.0 μmol of potassium ferricyanide in 33.3 μL of 50.0 mM sodium bicinate at pH 8.1; and 2 μmol of [2-^{14}C]pyruvate in 163 μL of water was added to initiate the reaction. After 25 s the reaction was quenched with acid. An additional experiment identical with that above was done in the presence of 0.5 mM GTP and 1.33 mM $MgCl_2$. The time of quench was the same.

A hybrid complex consisting of pyruvate dehydrogenase (E_1) from the PDH complex and the E_2E_3 subcomplex from the α-ketoglutarate dehydrogenase complex was prepared and tested for the presence of acetyl-TPP during steady-state decarboxylation and dehydrogenation of pyruvate. Purified pyruvate dehydrogenase (2.8 mg of E_1) was incubated with 4.1 mg of the E_2E_3 subcomplex prepared from the α-ketoglutarate dehydrogenase complex in a volume of 485 μL (20 mM sodium bicinate, pH 8.1) for a period of 30 min at room temperature. This amount of E_1 was equivalent to the E_1 present in the above experiments utilizing 6 mg of PDH complex. The amount of E_2E_3 subcomplex was consistent with the stoichiometry of 12:24:12 E_1:E_2:E_3 described by Reed (1974) for the α-ketoglutarate dehydrogenase complex. Three trapping experiments were done at room temperature rather

than 4 °C under otherwise identical conditions, and using the same procedures, as experiments with native PDH complex. The reactions were quenched at 2, 5, and 10 s.

The TPP-dependent, PDH complex catalyzed hydrolysis of acetyl-CoA described by CaJacob et al. (1985) was examined for the presence of acetyl-TPP in the steady state. Purified [1-^{14}C]acetyl-CoA was titrated to pH 6.0 with aqueous KOH prior to use. PDH complex (6 mg) was incubated at 4 °C with 2 μmol of NAD^+, 0.6 μmol of NADH, 0.4 μmol of TPP, and 1 μmol of $MgSO_4$ in a volume of 770 μL. The reaction was initiated by the addition of 0.5 μmol of [1-^{14}C]acetyl-CoA in a volume of 230 μL and allowed to progress for 1 min prior to quenching. A control reaction was run in the absence of TPP.

Following the acid quench, each reaction solution was treated as follows: The precipitation mixture was clarified by centrifugation and the supernate fluid applied to a 1.0 cm × 17 cm column of Sephadex SP-C25 that had been equilibrated with 30 mM HCl at 4 °C. The column was eluted with 30 mM HCl, and fractions 1.5 mL in volume were collected. The A_{260} and A_{310} of each fraction was recorded, and 50 μL from each fraction was diluted into 15 mL of liquid scintillation fluid together with 950 μL of water and counted in the liquid scintillation spectrometer. Those fractions having significant absorption at 310 nm (due to carrier acetyl-TPP) were pooled, giving approximately 15 mL, and concentrated by rotary evaporation to 4–5 mL.

Kinetic Measurements and Calculation of Rate Constants. The observed first-order rate constants for the hydrolysis of synthetic acetyl-TPP as a function of pH were found by following the decrease in A_{310} with time. A least-squares statistical analysis of ln $(A_t - A_\infty)$ versus time yielded the rate constants from the negative values of the slopes. The average of triplicate determinations was accepted as the rate constant. Temperature of the reaction was maintained at 24 °C, the pH was maintained by the presence of 50 mM buffer, and the ionic strength was adjusted to 0.5 M with NaCl. The following buffers were used over the indicated pH ranges: monobasic phosphate, pH 2.5–3.0; formate, pH 3.0–4.1; acetate, pH 4.1–5.5; MES, pH 5.5–6.7; and MOPS, pH 6.7–7.5. Five to twenty microliters of freshly prepared 20 mM acetyl-TPP was added to 995–980 μL of buffer solution to make 1 mL, the A_{310} was monitored to completion of the reaction, and then the pH of the reaction solution was recorded.

The first-order rate constants measured at pH values from 2.5 to 7.5 were fitted to eq 7 by a nonlinear regression analysis,

$$k_{obs} = C\frac{1 + K_2/[H^+]}{1 + [H^+]/K_1} \quad (7)$$

using a program supplied by W. W. Cleland. With the data in Figure 1, the fitting parameters in eq 7 were found to be $C = 0.125$, $K_1 = 1.82 \times 10^{-5}$, and $K_2 = 3.30 \times 10^{-7}$. These values were used to calculate the lines in Figures 1 and 6 and also to calculate rate constants at pH values other than those at which rate constants were measured.

The hydrolysis rate of synthetic acetyl-TPP was measured as a function of buffer concentration by using the buffer MOPS at pH 7.14 and acetate at pH 5.1. The experimental procedure and data analysis were as described above, except that ionic strength was adjusted to 2.0 M with NaCl. The range of buffer concentrations is shown in Table I.

The observed first-order rate constants for the hydrolysis of enzymatically produced [1-^{14}C]acetyl-TPP were found by measuring the production of [1-^{14}C]acetate as a function of time. Approximately 1 mL of the concentrated and purified TPP solution from the enzymatic reaction was diluted with water, 0.5–1.0 M buffer, and 0.75–1.0 M NaCl to bring the final volume to 2.6 mL and the ionic strength to 0.5 M. The buffers used were the same as for synthetic acetyl-TPP (see above). The recording of time was started immediately after the addition of buffer, with the temperature maintained at 24 °C by immersion in a temperature-controlled water bath. At appropriate times, aliquots of 500 μL were removed and quenched by dilution into 100 μL of 4 N H_2SO_4. This solution was transferred to one side of the volatile transfer vessel and frozen by immersion in 2-propanol/dry ice. Zero time points were made by adding in order the proportional amounts (with respect to the time point samples) of buffer, NaCl, 100 μL of 4 N H_2SO_4, H_2O, and sample to give 600 μL total volume. Once all reactions were complete and all samples frozen, each vessel was evacuated to approximately 2–4 torr while the sample side of the vessel was kept immersed in 2-propanol/dry ice. After evacuation, the exterior of the sample side was exposed to air while the volatile receptor side was immersed in 2-propanol/dry ice. All volatile substances in the reaction solution (i.e., H_2O and [1-^{14}C]acetic acid) were transferred within 2 h while the nonvolatile components of the reaction mixture (i.e., [1-^{14}C](1-hydroxyethyl)-TPP, [2-^{14}C]lactyl-TPP, unhydrolyzed [1-^{14}C]acetyl-TPP, [^{14}C]TPP carboligase products, and salts) remained in the sample side. The solution from the volatile receptor side (approximately 600 μL) was removed, the receptor side was washed with 400 μL of H_2O, and both the sample and wash were added to 15 mL of scintillation counting solution. The resulting solution was counted for 30 min in the ^{14}C window of the scintillation spectrometer.

The data for the production of [1-^{14}C]acetate from 2-([1-^{14}C]acetyl)-TPP were analyzed by statistical nonlinear regression analysis using the first-order rate equation:

$$B_t = B_0 + (A_0 - A_0E^{-kt}) \quad (8)$$

In this equation B_t represents [1-^{14}C]acetate at time t, B_0 is ^{14}C counts at time zero, A_0 is initial level of [1-^{14}C]acetyl-TPP, and k is the observed pseudo-first-order rate constant for the hydrolysis reaction.

Calculation of Percent E_1 Sites Occupied by ^{14}C-Labeled Acetyl-TPP, Hydroxyethyl-TPP, and Other [^{14}C]TPP-Labeled Products. The amounts of ^{14}C-labeled acetyl-TPP, hydroxyethyl-TPP, and other [^{14}C]TPP labeled products listed in Table II were calculated as follows. The number (in mmols) of TPP-E_1 sites was calculated for each experiment by using the molecular weights 5.0×10^6 for the PDH complex (accounting for 24 TPP-E_1 per molecule of complex) and 1.0×10^5 for isolated E_1. This value, which corresponded to the number of possible sites (100% labeling), was expressed as

Table I: Buffer Effects on Acetyl-TPP Hydrolysis[a]

buffer	concn (mM)	pH	k_{obs} (min^{-1})
acetate	50.0	5.1	0.0868
acetate	100.0	5.1	0.0868
acetate	200.0	5.1	0.0890
acetate	500.0	5.1	0.0892
MOPS	50.0	7.14	0.673
MOPS	100.0	7.14	0.680
MOPS	200.0	7.14	0.677
MOPS	500.0	7.14	0.672

[a] The concentration of buffer represents the total of both the protonated and deprotonated forms. For experiments in acetate buffer, 5 μL of acidic 20 mM acetyl-TPP was added to 995 μL of each buffer solution containing the appropriate amount of NaCl and HCl to make the final ionic strength 2.0 M and the pH 5.1. In the case of MOPS, the protocol was the same except for the higher pH and the addition of 20 μL of acidic 20 mM acetyl-TPP to 980 μL of buffer solution. Rate constants were determined as described under Experimental Procedure.

Table II: [1-^{14}C]Acetyl-TPP and Other TPP Adducts in Quenched Enzymatic Reactions[a]

expt no.	sample	trapped [^{14}C]TPP products (% of active sites)			
		acetyl-TPP	hydroxyethyl-TPP	other	total
1	PDH complex (complete)	0.431	19.2	9.7	29
2	PDH complex (anaerobic complete)	0.171	21.2	1.3	23
3	PDH complex + O_2 (-NAD^+)	2.38	56.7	11.0	70
4	PDH complex (-CoA)	0.479	45.5	0	46
5	PDH complex + GTP (complete)	0	72.0	20.0	91
6	PDH complex (-TPP)	0	0	0	0
7	PDH complex ([1-^{14}C]acetyl-CoA hydrolysis)	0.091	2.2	0	2.3
8	PDH complex (-TPP) ([1-^{14}C]acetyl-CoA hydrolysis)	0	0	0	0
9	E_1 + ferricyanide	2.78	36.3	6.4	46
10	E_1 + ferricyanide + GTP	12.0	58.8	25.0	96
11	hybrid complex (2 s)	0	22	0	22
12	hybrid complex (5 s)	0.344	16.9	0	17
13	hybrid complex (10 s)	0	14.1	0	14

[a] Trapping and volatile transfer procedures were as outlined under Experimental Procedures. Complete reactions contained [2-^{14}C]pyruvate, NAD^+, CoA, and TPP. Hydroxyethyl-TPP formed as a result of the rapid protonation by solvent of the enzymatic intermediate hydroxyethylidene-TPP.

microcuries by using the specific activity of [2-^{14}C]pyruvate or [1-^{14}C]acetyl-CoA. For acetyl-TPP, the percent sites filled was calculated from the total amount of ^{14}C associated with [1-^{14}C]acetyl-TPP in that sample (A_0 in eq 8) as estimated by nonlinear regression in the analysis of the hydrolysis rate. The ^{14}C radioactivity in the pooled concentrated sample not associated with [1-^{14}C]acetyl-TPP was assigned to [1-^{14}C]-hydroxyethyl-TPP, since these compounds overlap in elution volume (refer to Figure 5) upon chromatographic separation. These counts were then used in the calculation of percent sites filled for this ^{14}C-labeled molecule. The ^{14}C associated with other radioactive peaks eluting just prior to the pooled fractions was totaled and assigned as other TPP-labeled products.

Results

The pH–Rate Profile for Hydrolysis of Acetyl-TPP. The hydrolysis of acetyl-TPP accurately followed the first-order rate law throughout the pH range 2.5–7.5. The coefficient of variance in the calculated rate constants from regression analysis was less than 0.5%, and variation of the rate constant in triplicate determinations was less than 3.5% for all experiments. In addition, first-order kinetics at all pH values was confirmed by the finding that varying the starting concentrations of acetyl-TPP in otherwise identical reaction solutions gave the same rate constant. Inasmuch as no deviation from first-order behavior appeared by either method of rate measurement, the keto, hydrate, and carbinolamine forms of acetyl-TPP (Scheme II) were at equilibrium throughout all the hydrolysis reactions.

The pH–rate profile is shown by the *points* in Figure 1, where log k_{obs} for the hydrolysis of acetyl-TPP is plotted versus pH. The values of log k_{obs} increase with increasing pH in a complex relationship. This contrasts with the linear dependence upon activity of OH^- found in the hydrolysis of 2-acetyl-3,4-dimethylthiazolium ion studied by Lienhard (1966). In Figure 1 the slope is ~0.92 at pH values below 4. In the pH range of 5–6 the slope declines and then again increases at pH values above 6.5. The data in Table I show that the hydrolysis rate is not sensitive to buffer concentrations. Therefore, as in the case of the hydrolysis of 2-acetyl-3,4-dimethylthiazolium ion, the reaction is not subject to general acid–base catalysis.

The simplest explanation for the complex pH–rate profile is that it consists of two legs, both exhibiting first-order dependence on the activity of hydroxide, but displaced from each other in the interval of pH 4–6 because of an ionization within acetyl-TPP at a site remote from the acetyl group. This site

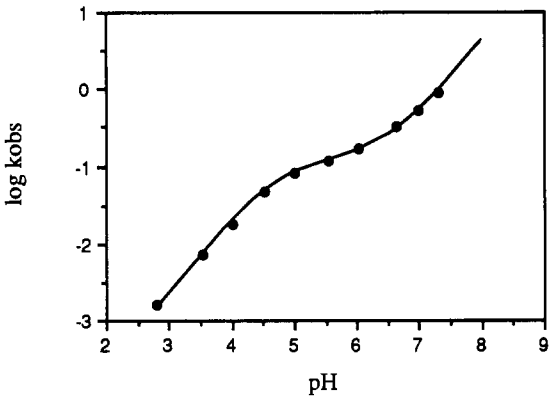

FIGURE 1: pH–rate profile for the hydrolysis of acetyl-TPP. The log of the first-order rate constant for the hydrolysis of acetyl-TPP is plotted as a function of pH at 24 °C. Each data point represents the average of triplicate determinations (coefficient of variance <3.5%). The data points were fitted to eq 7 as described under Experimental Procedures, and the resulting parameters were used to calculate the line shown in the figure.

is one associated with a pK_a near 5 and is almost certainly the dissociation of the proton from the pyrimidinium ring. Such a kinetic model is shown in Figure 2, where the two protonation levels for acetyl-TPP are the pyrimidinium forms shown in Scheme I and the pyrimidine forms that result from loss of a proton, all of which are at equilibrium. The immediate cleavage intermediates are the anions of the hydrates at the two pyrimidine protonation levels, which decompose to acetic acid and $TPPH^+$ or TPP with rate constants of k_1 and k_2, respectively. The observed first-order rate constant for the hydrolysis of acetyl-TPP, based on this kinetic model, is given by eq 9, where K_1 and K_2 are given by eq 9a and 9b, respectively.

$$k_{obs} = \frac{k_2K_2K_a + k_1K_1[H^+]}{K_2K_a + (K_1 + K_a)[H^+] + [H^+]^2} \quad (9)$$

$$K_1 = \frac{K_{1c}K_{1h}K_{1i}}{1 + K_{1c} + K_{1c}K_{1h}} \quad (9a)$$

$$K_2 = \frac{K_{2c}K_{2h}K_{2i}}{1 + K_{2c} + K_{2c}K_{2h}} \quad (9b)$$

Insufficient data are available to obtain reliable estimates of all the rate and equilibrium constants in this mechanism. However, the pH–rate profile is consistent with this mechanism; and independent information also supports the mechanism. The data points in Figure 1, fitted as described under

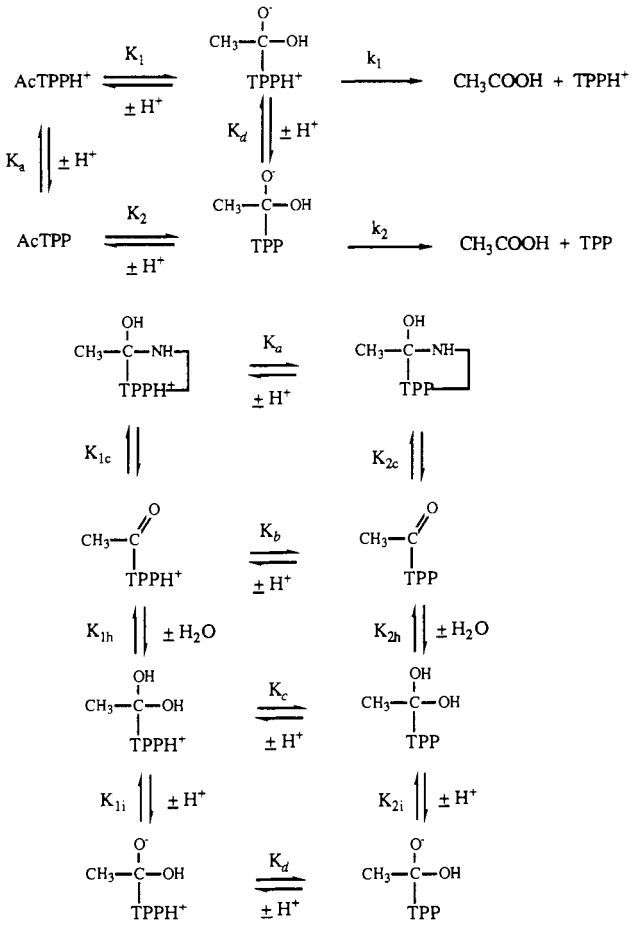

FIGURE 2: Kinetic model for the hydrolysis of acetyl-TPP.

Experimental Procedures, give the following values: pK_a = 4.73 ± 0.13 (SE); $k_1K_1 = (2.28 \pm 0.09) \times 10^{-6}$; and $k_2K_2 = (4.12 \pm 0.22) \times 10^{-8}$. The *line* in Figure 1 is calculated by using these parameters. K_a is the acid dissociation constant for the pyrimidinium ring in the three forms of acetyl-TPP. This dissociation is coupled to a shift in the partitioning of acetyl-TPP among its three molecular forms shown in Scheme II. This shift can be observed by the dependence of A_{320} and A_{290} on pH. The keto form of acetyl-TPP exhibits an absorption maximum at 310 nm, and the carbinolamine band appears as a shoulder at 280 nm (Gruys et al., 1987). The plots of A_{320} and A_{290} versus pH in Figure 3 show that the concentration of the keto form decreases as the pH increases above 4.5, and the concentration of the carbinolamine form correspondingly increases. This transition is associated with the loss of a proton from the pyrimidinium ring. The value of this pK_a in the case of TPP is 4.8 (Cain et al., 1977). The data points in Figures 3, panels A and B, when fitted to a dissociation equation, correspond to pK_a values of 4.90 ± 0.03 (A_{320}) and 5.07 ± 0.09 (A_{290}). These data were obtained at 4 °C to minimize the hydrolysis of acetyl-TPP during the measurement, and so the values differ slightly from the kinetic value of 4.73 because of the effects of temperature on the equilibria. Nevertheless, the data in Figure 3 support the mechanism and the assignment of K_a.

The characteristic shape of the pH–rate profile is due to the fact that k_1K_1 is larger than k_2K_2 by a factor of 55. These are complex constants and can in principle have their relative values for any of several reasons. The relationship between them can be understood to result from the expection that k_1 should be larger than k_2, since the pyrimidine-protonated form of TPP should be a better leaving group than the unprotonated

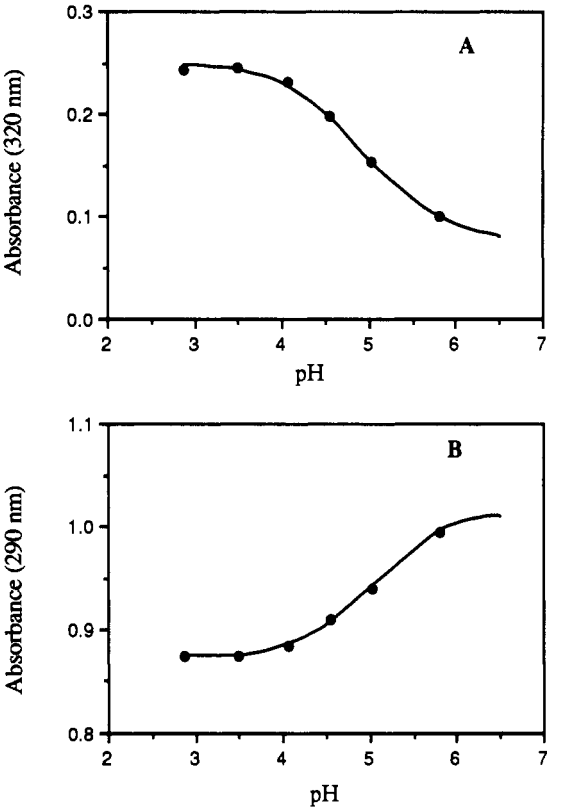

FIGURE 3: Ionization of the aminopyrimidinium moiety of acetyl-TPP. The values of A_{320} and A_{290} for acetyl-TPP were measured for a solution of acetyl-TPP as a function of pH and fitted to a dissociation equation. The procedure is described under Experimental Procedures. The decrease in A_{320} and increase in A_{290} with pH reflect the repartitioning of the three forms of acetyl-TPP to favor the carbinolamine at pH values above 5. The pK_a values for the curves shown are 4.90 ± 0.03 (A_{320}) and 5.09 ± 0.09 (A_{290}).

form. Moreover, independent evidence proves that K_1 is larger than K_2. This evidence is the pH dependence of A_{320} and A_{290} in Figure 3, which shows that the partitioning of acetyl-TPP favors the carbinolamine at pH values above 5; that is, $K_{1c} \gg K_{2c}$ in eq 9a and 9b. This is further supported by the proton NMR spectrum in Figure 4, showing that at pD 6.0 approximately 75% of acetyl-TPP is the carbinolamine. In contrast, under acidic conditions at pD 1.3 the three forms are more nearly equally partitioned, with the levels of the hydrate and carbinolamine approximately equal and about half the concentration of the keto form (Gruys et al., 1987). The values of K_{1h} and K_{2h} are both near unity, as shown by the proton NMR spectra; and K_{1i} should either be comparable to K_{2i} or larger owing to the inductive effect of the pyrimidinium ring. This inductive effect lowers the pK for the dissociation of the 2-H in TPP by 0.4 (Washabaugh & Jencks, 1988). The effect should be smaller but in the same direction for the hydrate of acetyl-TPP. All of these factors contribute to the fact that K_1 is larger than K_2. Consequently, most of the acetyl-TPP is in the carbinolamine form above pH 5, and the concentration of the hydrate anion is much lower than it would be at that pH if there were no shift to the carbinolamine upon deprotonation of the pyrimidinium ring; that is, if partitioning of acetyl-TPP among its three forms remained the same as in acidic solutions. Since $K_1 > K_2$ and $k_1 > k_2$, it must be that $K_1k_1 > K_2k_2$, and this explains the shape of the pH-rate profile.

Trapping of [1-^{14}C]Acetyl-TPP. Cation-exchange chromatography using Sephadex SP-C25 under acidic conditions (pH 1.5) is a useful means of separating TPP from adducts of TPP that exist in the acid quench of enzymatic reaction

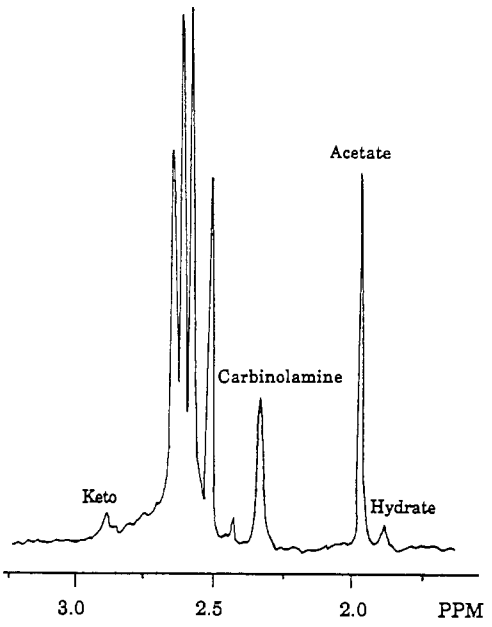

FIGURE 4: ^{1}H NMR spectrum of acetyl-TPP at pD 6. The spectrum was recorded 6 min after preparing the solution at pD 6.0 and 24 °C. The total acquisition time was 2 min (100 scans at 1.2 s/scan). A 20 mM sample, originally in 0.75 mL of 100 mM DCl in D_2O, was titrated in the NMR tube to pD 6.0 by using 35 μL of 1.0 M dipotassium phosphate dissolved in D_2O. The amount of cleavage during manipulation of the sample, as measured by acetate production and integration of peaks, is about 50%. Labeled peaks are to the acetyl methyl group protons of acetyl-TPP except for the one marked acetate. Assignments are based on data from Gruys et al. (1987).

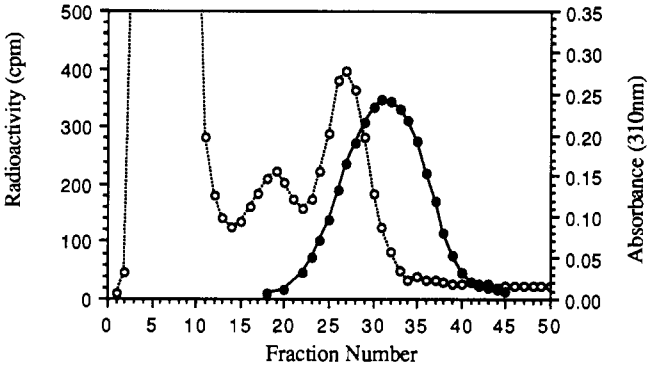

FIGURE 5: Chromatography of [1-^{14}C]acetyl-TPP. Shown is an elution profile for the purification of enzymatically produced ^{14}C-labeled TPP derivatives after the reaction had been quenched with acid. The solid phase was a Sephadex SP-C25 column (1.0 × 17 cm) equilibrated and eluted with 30 mM HCl. The open symbols are radioactivity and the closed symbols are A_{310}. The assignment of peaks is discussed in the text.

solutions. Figure 5 is a typical elution profile for the chromatographic purification of ^{14}C-labeled TPP products. Substrates, products, and cofactors are eluted within 16 fractions after loading of the sample. Peaks that appear after fraction 16 are TPP and TPP adducts, which are positively charged under these conditions. They are identified by their characteristic UV–vis absorption spectra and cochromatography with authentic samples. The elution order of TPP and TPP adducts with SP-C25 chromatography are lactyl-TPP and acetolactyl-TPP, followed by hydroxyethyl-TPP, acetyl-TPP, and TPP. The first two are not separated, and the latter three compounds are not completely separated. Acetyl-TPP in particular emerges in a broad peak overlapping both hydroxyethyl-TPP and TPP, presumably owing to the fact that it is a mixture of three species. In the radioactivity elution profile, the peak appearing between fractions 15 and 20 is

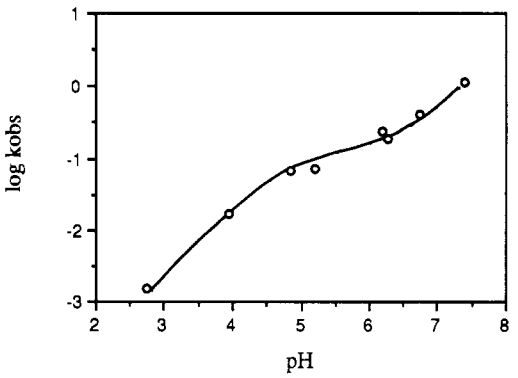

FIGURE 6: pH–rate profile for hydrolysis of [1-^{14}C]acetyl-TPP isolated from enzymatic reactions. Plotted as points are the log k_{obs} as a function of pH for appearance of volatile ^{14}C counts from acid quenched steady-state TPP products produced by pyruvate dehydrogenase catalyzed reactions. The line is calculated by using the fitting parameters derived from the data in Figure 1.

lactyl-TPP and/or acetolactyl-TPP. Since lactyl-TPP undergoes decarboxylation under the conditions of these experiments (Kluger et al., 1981), most of the radioactivity appearing in this peak is probably the carboligase product and is assigned as "other" in Table II. The major peak appearing between fractions 22 and 30 is hydroxyethyl-TPP. Radioactivity appearing beyond fraction 32 is due to acetyl-TPP, which appears in a broad peak extending from fraction 22 to fraction 40, as shown by the profile of A_{310} due to carrier acetyl-TPP. In the trapping experiments the pooled fractions exhibiting A_{310} contain both [1-^{14}C]acetyl-TPP and [1-^{14}C]hydroxyethylidene-TPP.

The pooled ^{14}C-containing fractions can be analyzed for [1-^{14}C]acetyl-TPP by exploiting its characteristic chemical lability to hydrolysis. Upon hydrolysis the [1-^{14}C]acetic acid can be isolated by sublimation and radiochemically assayed, while the unreactive and nonvolatile [1-^{14}C]hydroxyethyl-TPP remains behind. The hydrolysis can be conducted at any desired pH, and the rate can be measured by analysis for [1-^{14}C]acetic acid as a function of time. The resulting rate constants characterize [1-^{14}C]acetyl-TPP, since the pH–rate profile for acetyl-TPP is known from Figure 1. Shown as *points* in Figure 6 is the pH–rate profile for the hydrolysis of [1-^{14}C]acetyl-TPP obtained in enzymic trapping experiments. The *line* in Figure 6 is calculated from the fitting parameters derived from the data in Figure 1. It is clear that the pH–rate profile for hydrolysis of the putative [1-^{14}C]acetyl-TPP, isolated as a minor component in admixture with [1-^{14}C]-hydroxyethylidene-TPP, is identical with that of authentic acetyl-TPP.

Table II presents results obtained in a series of trapping experiments as the percent of E_1 active sites filled with the indicated species in the steady state. The levels of these species varied significantly depending on reaction conditions. In control experiments in which TPP was omitted from the reaction mixture, no ^{14}C-labeled products could be detected. Therefore, the ^{14}C products are not simply artifactual; and our enzyme preparations contained no active, tightly bound TPP. In general, [1-^{14}C]acetyl-TPP could easily be detected in any reaction mixture that contained enzyme, TPP, and a ^{14}C-labeled substrate. When the substrate was [2-^{14}C]pyruvate, an oxidizing agent was also required, and O_2 could serve this purpose. With [1-^{14}C]acetyl-CoA as the substrate no oxidizing agent was required; but NADH was required as well as TPP, as in the TPP- and NADH-depenent hydrolysis of acetyl-CoA (CaJacob et al., 1985).

For the PDH complex catalyzing the overall reaction of eq

6, [1-^{14}C]acetyl-TPP is present in the steady state in significant amounts under conditions in which the reaction is proceeding in either aerobic or anaerobic conditions. When NAD^+ is omitted (experiment 3), the only oxidizing agent present other than lipoyl groups is oxygen gas. Oxygen can oxidize [1-^{14}C]hydroxyethylidene-TPP and generates a level of [1-^{14}C]acetyl-TPP that is comparable with that prevailing when E_1 alone catalyzes the decarboxylation in the presence of ferricyanide as the oxidizing agent. In the absence of CoA (experiment 4) the reaction proceeds to the stage of the reductive [1-^{14}C]acetylation of lipoyl groups on E_2 according to eq 2, which quickly reaches equilibrium. The equilibrium state contains a substantial amount of [1-^{14}C]acetyl-TPP. In the presence of GTP, an allosteric inhibitor or, in the absence of TPP (experiments 5 and 6), no [1-^{14}C]acetyl-TPP can be observed.

The hybrid complex formed between E_1 of the PDH complex and the E_2E_3 subcomplex from the α-ketoglutarate dehydrogenase complex also catalyzes eq 6 but at a much slower rate (Steginsky et al., 1984). By use of this complex (experiments 11–13) the [1-^{14}C]acetyl-TPP appears transiently and disappears at the conclusion of the reaction.

The two experiments in which the effects of GTP, an allosteric inhibitor (Schwartz & Reed, 1970), on the levels of intermediates were investigated present some interesting insights into the action of GTP. The effect of GTP acting as an inhibitor of the overall reaction (eq 6) enhances the levels of hydroxyethyl-TPP and TPP species other than acetyl-TPP, which is undetectable. The effect of GTP on E_1 itself, when ferricyanide is the electron acceptor, is in one sense similar to its effect on the overall reaction involving all three enzymes; however, in another sense it is very different. On one hand GTP enhances the levels of hydroxyethyl-TPP and other TPP species, as in the overall reaction. On the other hand, GTP dramatically enhances the level of acetyl-TPP in the steady state, in marked contrast to its effect on the overall reaction.

The apparent paradox in the effects of GTP can be understood on the basis that it decreases the forward rates of *all* the reaction steps catalyzed by E_1. This can result from the energy made available by GTP binding being used to maintain the enzyme in a conformation that is suboptimal for catalysis of all the reaction steps in which E_1 plays an important role. Since E_2 is unaffected by GTP, any intermediate that interacts with E_2 can be decomposed at the usual rate. But its rate of *formation* is reduced by GTP. This means that the steady-state level of any such intermediate will be dramatically reduced by GTP, as is observed for acetyl-TPP in experiment 5 of Table II.

The situation with the steady-state level of acetyl-TPP in experiments 9 and 10 of Table II, with E_1 and ferricyanide, is quite different. Here the effect of GTP as an inhibitor of all E_1 functions leads to a very large increase in the steady-state level of acetyl-TPP, as well as enhanced levels of the other TPP species. The level of hydroxyethyl-TPP, while increased by GTP, is not as high as in the overall reaction. These results indicate that GTP does not inhibit the oxidation of hydroxyethylidene-TPP by ferricyanide, which is probably simply a chemical oxidation that allows acetyl-TPP to be formed at a rate that is independent of the presence of GTP. But GTP evidently inhibits the hydrolysis of acetyl-TPP and thereby leads to a substantial enhancement in the steady-state level of acetyl-TPP.

According to this rationale, catalysis of the hydrolysis of acetyl-TPP is a function of E_1 that is subject to inhibition by GTP. Hydrolysis of acetyl-TPP is not a step in the overall reaction catalyzed by the PDH complex (eq 1–5). However, this hydrolysis may be mechanistically related to one or more of the steps in the reductive acetylation of lipoyl groups by hydroxyethylidene-TPP (eq 2); and it may require a similar catalytic involvement by E_1.

Discussion

pH–Rate Profile for Acetyl-TPP. The principle findings in the present work are that the pH dependence for the hydrolysis of acetyl-TPP is more complex than that of the model compound 2-acetyl-3,4-dimethylthiazolium ion. The complexities are explained by the existence of acetyl-TPP in three molecular forms, by the effects of pH on the partitioning among these forms, and very likely by the differential inductive effects of the pyrimidinium and pyrimidine groups on the acid dissociation constants for the hydrate forms (K_{1i} and K_{2i} in Figure 2). The hydrolysis of 2-acetyl-3,4-dimethylthiazolium ion proceeds with specific-base catalysis (Lienhard, 1966). The hydrolysis of acetyl-TPP is more complex, although it too involves specific-base catalysis. The two legs of the pH–rate profile in Figure 1 are displaced by the effects of the pK_a for the pyrimidinium ring of acetyl-TPP. The complex pH–rate profile serves to characterize acetyl-TPP and is exploited in this work to identify [1-^{14}C]acetyl-TPP isolated in quenched enzymatic reactions of [2-^{14}C]pyruvate and [1-^{14}C]acetyl-CoA.

Washabaugh and Jencks (1988) recently investigated the possibility that the aminopyrimidine ring of TPP may be an intramolecular catalyst for the ionization of the 2-C(H) proton in the thiazolium ring. They found no evidence for such catalysis. The proximity of the aminopyrimidinyl moiety to the 2-C(H) is evidently insufficient for it to compete with solvent at this position. In the case of acetyl-TPP, however, the aminopyrimidine group is clearly sufficiently proximal to the acetyl group to compete with water for addition to the carbonyl group, and it even outcompetes water at pH values above 5. This observation does not justify any conclusion that the aminopyridine interacts with the acetyl or hydroxyethylidene groups of TPP intermediates at the active site of any enzyme. However, it is clear that such interaction, perhaps as a catalyst for proton transfer to and from the carbonyl oxygen, should be considered to be possible. The cyclic carbinolamine form of acetyl-TPP does not itself seem to offer any advantage in catalysis by TPP; and this species is not considered likely to be an intermediate in enzymatic reactions.

Identification of Enzymatically Produced Acetyl-TPP. Our earlier research on the synthesis, characterization, and properties of acetyl-TPP made it possible to design experiments leading to the trapping of acetyl-TPP from enzymatic reactions. The fact that acetyl-TPP is stable in acid verified that an acid quench should be a suitable means of arresting reactions employing ^{14}C-labeled substrates. The availability of authentic acetyl-TPP allowed the development of methods for isolating and detecting it as carrier from quenched reaction mixtures. And the pH–rate profile for its hydrolysis made possible the positive identification of [1-^{14}C]acetyl-TPP as a minor component of the ^{14}C-labeled TPP-containing species isolated. This compound and the methods here described for isolating it from the enzymatic reaction solution and identifying it should prove to be applicable to studies of other enzymes in which it is likely to be an intermediate.

Acetyl-TPP as an Intermediate in Reactions Catalyzed by Pyruvate Dehydrogenase. Acetyl-TPP has long been regarded as a probable intermediate in the decarboxylation and dehydrogenation of pyruvate catalyzed by the E_1 component of the PDH complex with ferricyanide acting as the electron acceptor, which is believed to follow the course of eq 10–13. The

$$\text{pyruvate} + E_1\text{–TPP} \rightleftharpoons E_1\cdot\text{lactyl-TPP} \quad (10)$$

$$E_1\cdot\text{lactyl-TPP} \rightarrow E_1\cdot\text{hydroxyethylidene-TPP} + CO_2 \quad (11)$$

$$E_1\cdot\text{hydroxyethylidene-TPP} + 2Fe(CN)_6^{-3} \rightleftharpoons E_1\cdot\text{acetyl-TPP} + 2Fe(CN)_6^{-4} + H^+ \quad (12)$$

$$E_1\cdot\text{acetyl-TPP} + H_2O \rightarrow E_1\cdot\text{TPP} + \text{acetate} + H^+ \quad (13)$$

present work has confirmed this expectation with the results of experiment 9 of Table II, in which 2.78% of the E_1 sites were found to be occupied by acetyl-TPP in the steady state. This experiment further served to establish a framework in which the results of other trapping experiments could be evaluated, by showing that the steady-state level of acetyl-TPP should be expected to be low, even in cases in which it is virtually certain to be an intermediate. The lower levels of acetyl-TPP found with the PDH complex catalyzing the overall reaction had to be accepted as reasonable levels for an intermediate, given what is independently known about this system. In particular, Flournoy and Frey (1987) found that >96% of acetyl-TPP generated at the active site of E_1 from fluoropyruvate could be prevented from reacting with water by the presence of dihydrolipoamide, the acetyl groups being transferred instead to dihydrolipoamide. This meant that acetyl-TPP reacted faster with dihydrolipoamide at the E_1 active site than with water. Therefore, the steady-state level of acetyl-TPP in experiments 1 and 2 of Table II had to be expected to be lower than that in experiment 9, since in the overall reaction (experiments 1 and 2) any acetyl-TPP generated at the E_1 active site would exist in the presence of dihydrolipoyl groups. In experiment 9, with ferricyanide as the electron acceptor and no E_2, only water was present and available to act as the acetyl group acceptor, so that deacetylation was slower than in the overall reaction; and the steady-state level of acetyl-TPP was consequently elevated.

The present results show that acetyl-TPP is transiently formed in the overall reaction catalyzed by the PDH complex (eq 6). It is most likely generated as a transient species in eq 2. Whether acetyl-TPP is a compulsory intermediate cannot be decided on the available evidence, since acetyl-TPP might be in equilibrium with the dihydrolipoyl–acetyl-TPP tetrahedral adduct in Scheme II, rather than an obligatory intermediate in the formation of the tetrahedral adduct. In any case pathway B in Scheme II cannot be excluded by the present results and must be considered to be a viable alternative to pathway A.

Earlier experiments also indicated the competency of acetyl-TPP as an intermediate. CaJacob et al. (1985) found that the PDH complex catalyzes the hydrolysis of acetyl-CoA in a reaction that requires all three enzymes, NADH, TPP, and the lipoyl groups of E_2. Hydrolysis was explained on the basis that reversal of the overall reaction to the reductive acetylation (eq 2) led to the formation of a low equilibrium concentration of acetyl-TPP, which then underwent hydrolysis to acetate. Experiment 7 in Table II, which was carried out under similar reaction conditions, showed that [1-^{14}C]acetyl-TPP is indeed generated under these conditions. A small amount of [1-^{14}C]hydroxyethyl-TPP was also found, and this probably resulted from partial reduction of acetyl-TPP by the dihydrolipoyl groups also present on E_2 and generated by NADH and E_3 under these reaction conditions.

Now that acetyl-TPP is known to be present in the steady state of the overall pyruvate dehydrogenase reaction, the question of its origin must be addressed. Is it formed in an equilibrium side reaction from the tetrahedral adduct in Scheme I, which in turn is generated by pathway A, the tightly coupled pathway in which hydroxyethylidene-TPP reacts as a carbanion with lipoic acid? Or is acetyl-TPP a compulsory intermediate lying on pathway B of Scheme I and an obligatory intermediate on the pathway to the formation of the tetrahedral adduct? The answer to this question must now be found by defining the connection between hydroxyethylidene-TPP and the tetrahedral adduct, since several series of experiments, including the present work, have failed to discredit acetyl-TPP as an intermediate.

Acknowledgments

We thank Professor W. W. Cleland for valuable assistance with fitting the data of Figures 1, 3, and 6 and Professor R. H. Kluger for the generous gift of a sample of lactyl-TPP.

References

Breslow, R. (1958) *J. Am. Chem. Soc. 80*, 3719–3726.
Breslow, R., & McNelis, E. (1960) *J. Am. Chem. Soc. 82*, 2394–2395.
Bunton, C. A., & Shiner, V. J., Jr. (1961) *J. Am. Chem. Soc. 83*, 3207–3214.
Cain, A. H., Sullivan, G. R., & Roberts, J. D. (1977) *J. Am. Chem. Soc. 99*, 6423–6425.
CaJacob, C. A. (1984) Doctoral Dissertation, The Ohio State University.
CaJacob, C. A., Gavino, G. R., & Frey, P. A. (1985) *J. Biol. Chem. 260*, 14610–14615.
da Foneseca-Wollheim, F., Bock, K. W., & Holzer, H. (1962) *Biochem. Biophys. Res. Commun. 9*, 466–471.
Daigo, K., & Reed, L. J. (1962) *J. Am. Chem. Soc. 84*, 659–662.
Das, M. L., Koike, M., & Reed, L. J. (1961) *Proc. Natl. Acad. Sci. U.S.A. 47*, 753–759.
Flournoy, D. S., & Frey, P. A. (1986) *Biochemistry 25*, 6036–6043.
Gold (1956) *pH Measurements*, p 120, Methuen, London.
Goldberg, M. L., & Racker, E. (1962) *J. Biol. Chem. 237*, 3841–3842.
Gruys, K. J., Halkides, C. J., & Frey, P. A. (1987) *Biochemistry 26*, 7575–7585.
Holzer, H., & Beaucamp, K. (1961) *Biochim. Biophys. Acta 46*, 225–243.
Kluger, R., Chin, J., & Smyth, T. (1981) *J. Am. Chem. Soc. 103*, 884–888.
Lienhard, G. E. (1966) *J. Am. Chem. Soc. 88*, 5642–5649.
Lipmann, F., & Tuttle, L. C. (1945) *J. Biol. Chem. 159*, 21–28.
Pettit, F. H., Hamilton, L., Munk, P., Namihira, G., Eley, M. H., Willms, C. R., & Reed, L. J. (1973) *J. Biol. Chem. 248*, 5282–5290.
Reed, L. J. (1974) *Acc. Chem. Res. 7*, 40–46.
Reed, L. J., & Willms, C. R. (1969) *Methods Enzymol. 9*, 247–265.
Reed, L. J., & Mukherjee, B. B. (1969) *Methods Enzymol. 13*, 55–61.
Rose, I. A., Grunberg-Manago, M., Korey, S. R., & Ochoa, S. (1954) *J. Biol. Chem. 211*, 737–756.
Schroter, W., & Holzer, H. (1963) *Biochim. Biophys. Acta 77*, 474–481.
Schwartz, E. R., & Reed, L. J. (1970) *Biochemistry 9*, 1434–1439.
Speckhard, D. C. (1975) Doctoral Dissertation, The Ohio State University.
Speckhard, D. C., & Frey, P. A. (1975) *Biochem. Biophys. Res. Coommun. 62*, 614–620.
Steginsky, C. A., & Frey, P. A. (1984) *J. Biol. Chem. 259*, 4023–4026.

Steginsky, C. A., Gruys, K. J., & Frey, P. A. (1985) *J. Biol. Chem. 260*, 13690–13693.
Washabaugh, M. W., & Jencks, W. P. (1988) *Biochemistry 27*, 5044–5053.
White, F. G., & Ingraham, L. L. (1960) *J. Am. Chem. Soc. 82*, 4114–4115.
White, F. G., & Ingraham, L. L. (1962) *J. Am. Chem. Soc. 84*, 3109–3111.

Spectroelectrochemical Studies of the Corrinoid/Iron–Sulfur Protein Involved in Acetyl Coenzyme A Synthesis by *Clostridium thermoaceticum*†

Scott R. Harder, Wei-Ping Lu, Benjamin A. Feinberg, and Stephen W. Ragsdale*
Department of Chemistry, The University of Wisconsin—Milwaukee, Milwaukee, Wisconsin 53201
Received January 19, 1989; Revised Manuscript Received June 30, 1989

ABSTRACT: An 88-kDa corrinoid/iron–sulfur protein (C/Fe-SP) is the methyl carrier protein in the acetyl-CoA pathway of *Clostridium thermoaceticum*. In previous studies, it was found that this C/Fe-SP contains (5-methoxybenzimidazolyl)cobamide and a $[4Fe\text{-}4S]^{2+/1+}$ center, both of which undergo redox cycling during catalysis, and that the benzimidazole base is uncoordinated to the cobalt (base off) in all three redox states, 3+, 2+, and 1+ [Ragsdale, S. W., Lindahl, P. A., & Münck, E. (1987) *J. Biol. Chem. 262*, 14289–14297]. In this paper, we have determined the midpoint reduction potentials for the metal centers in this C/Fe-SP by electron paramagnetic resonance and UV–visible spectroelectrochemical methods. The midpoint reduction potentials for the $Co^{3+/2+}$ and the $Co^{2+/1}$ couples of the corrinoid were found to be 300–350 and −504 mV (±3 mV) in Tris-HCl at pH 7.6, respectively. We also removed the (5-methoxybenzimidazolyl)cobamide cofactor from the C/Fe-SP and determined that its $Co^{3+/2+}$ reduction potential is 207 mV at pH 7.6. The midpoint potential for the $[4Fe\text{-}4S]^{2+/1+}$ couple in the C/Fe-SP was determined to be −523 mV (±5 mV). Removal of this cluster totally inactivates the protein; however, there is little effect of cluster removal on the midpoint potential of the $Co^{2+/1+}$ couple. In addition, removal of the cobamide has an insignificant effect on the midpoint reduction potential of the [4Fe-4S] cluster. A 27-kDa corrinoid protein (CP) also was studied since it contains (5-methoxybenzimidazolyl)cobamide in the base-on form. The reduction potentials for the $Co^{3+/2+}$ and $Co^{2+/1+}$ couples of the 27-kDa CP were found to be 215 and −630 mV, respectively, at pH 7.6. Our work provides evidence that the C/Fe-SP stabilizes the active Co^{1+} state of the C/Fe-SP relative to that of the 27-kDa CP and free corrinoids by control of the state of ligation of the benzimidazole base to Co^{2+}. The implications of this increased stability in the context of the methyl-transfer reaction catalyzed by this enzyme are discussed. Our results are consistent with a mechanism of methyl transfer to CO dehydrogenase in which a nucleophile on CODH performs a heterolytic displacement of the methyl group of the methylCo^{3+} corrinoid, resulting in Co^{1+} and methylated CODH.

The Wood pathway of acetyl-CoA synthesis is an autotrophic pathway of anaerobic growth [see Wood et al. (1986a,b), Ljungdahl (1986), and Fuchs (1987) for recent reviews]. The pathway recently has been found to occur in a number of anaerobic organisms, from acetogenic and sulfate-reducing eubacteria to methanogenic archebacteria (Wood et al., 1986a,b; Fuchs, 1987). The acetogenic bacteria use the pathway for generation of cell carbon and energy from CO, CO_2/H_2, or organic substrates and synthesize acetate as the major fermentation product. The methanogens use the pathway for synthesis of cell carbon and also for acetoclastic synthesis of methane. The Wood pathway is a unidirectional synthesis of a two-carbon compound, acetate, from two one-carbon precursors. The pathway is outlined in Figure 1, which emphasizes the role of the C/Fe-SP in the pathway. First, methyl-H_4 folate is formed from CO_2 in reactions involving formate dehydrogenase and tetrahydrofolate- (H_4folate) dependent enzymes (Ljungdahl, 1986). Then, the methyl group of methyl-H_4folate is transferred to a corrinoid/iron–sulfur protein (C/Fe-SP), forming a methyl-Co cobamide, in a reaction catalyzed by methyltransferase (MeTr) (Drake et al., 1981; Hu et al., 1984; Ragsdale et al., 1987). Next, CO_2 (after reduction) or CO reacts with CO dehydrogenase (CODH) to form an organometallic mixed-metal center consisting of Ni, two to three Fe, and CO (Ragsdale et al., 1986). Then, the methyl group of the methylated C/Fe-SP is transferred to CODH, apparently forming a methylcysteine intermediate (Pezacka & Wood, 1988), CoA binds, and CODH catalyzes the formation of acetyl-CoA from the bound methyl, CO, and CoA groups (Ragsdale & Wood, 1985).

We are interested in understanding the methyl-transfer reactions to the C/Fe-SP from methyl-H_4folate and from the methylated C/Fe-SP to CODH. The C/Fe-SP is an 88-kDa protein which was isolated from *Clostridium thermoaceticum* and was shown to act as a methyl carrier in the acetyl-CoA pathway, and an enzyme-bound methylcobamide was identified (Hu et al., 1984). Subsequently, the C/Fe-SP was purified to homogeneity and the metal sites in the protein were studied by EPR, Mössbauer, and UV–visible spectroscopy (Ragsdale et al., 1987). The C/Fe-SP contains a corrinoid, (5-methoxybenzimidazolyl)cobamide, and a $[4Fe\text{-}4S]^{2+/1+}$ cluster, both of which undergo redox changes during the reaction cycle of

† This work was supported by grants to S.W.R. from the National Institutes of Health (GM39451) and the Milwaukee Foundation (Shaw Scholars Fund).
* Address correspondence to this author at the Department of Chemistry, P.O. Box 413, College of Letters and Sciences, The University of Wisconsin—Milwaukee, Milwaukee, WI, 53201.

0006-2960/89/0428-9080$01.50/0